Geological Quarterly, 2025, 69, 32
DOI: https://doi.org/10.7306/gq.1805

Petrogenesis of metabasite olistoliths from the Magura Nappe in the Polish Western Outer Carpathians

Marek CIESZKOWSKI[1], Anna WOLSKA[2], Mateusz SZCZĘCH[1, *], Andrzej ŚLĄCZKA[1], Maciej KANIA[1], Robert ANCZKIEWICZ[3], Marek SZCZERBA[3] and Zuzanna CIESIELSKA[3]

[1] Jagiellonian University, Institute of Geological Sciences, Gronostajowa 3a, 30-387 Kraków, Poland; ORCID: 0000-0003-2176-239X [M.C.], 0000-0001-9089-7947 [M.S.], 0000-0002-3902-294X [A.Ś.], 0000-0001-5307-4714 [M.K.]

[2] University of the National Education Commission, Institute of Biology and Earth Sciences, Podchorążych 2, 30-084 Kraków, Poland; ORCID: 0000-0002-8596-5009 [A.W.]

[3] Polish Academy of Sciences, Institute of Geological Sciences, Poselska 1, 31-002 Kraków, Poland; ORCID: 0000-0001-6541-5192 [R.A.], 0000-0002-0485-886X [M.S.], 0000-0002-3749-5874 [Z.C.]

Cieszkowski, M., Wolska, A., Szczęch, M., Ślączka, A., Kania, M., Anczkiewicz, R., Szczerba, M., Ciesielska, Z., 2025. Petrogenesis of metabasite olistoliths from the Magura Nappe in the Polish Western Outer Carpathians. Geological Quarterly, 69, 32; https://doi.org/10.7306/gq.1805

Associate Editor: Jacek Szczepański

We provide new geochemical and geochronological data on metabasite blocks exposed in the Osielczyk Stream within the Polish Western Outer Carpathians. These blocks, the only known occurrence of this rock type in the Carpathian flysch, form part of an olistostrome within the flysch deposits of the Pasierbiec Sandstone Formation of the Magura Nappe. The metabasites are dark green, medium-grained, deformed rocks containing porphyroclasts of albite and Mg-hornblende, with secondary minerals (phengite and chlorite) defining the foliation. Bulk geochemical analyses reveal moderate contents of Fe_2O_3, MgO, TiO_2, P_2O_5 and transition elements (Cr, Ni, Co and V), alongside low concentrations of high field strength elements (HFSEs: Zr, Hf, Th, U), large ion lithophile elements (LILEs: Sr, Ba, K, Rb), and total rare earth elements (REE: 95.5–92.3 ppm). Chondrite-normalized ratios include $(La/Sm)_n$ = 2.4–2.3 and $(Tb/Yb)_n$ = 1.3–1.2, with a slightly negative Eu anomaly (Eu/Eu* = 0.83–0.91). The chemical composition corresponds to basaltic andesite or andesite magma, exhibiting intermediate characteristics between arc tholeiite and calc-alkaline series. These metabasites resemble high-alumina basalts (maximum Al_2O_3 content 18.6 wt.%) and display geochemical signatures akin to volcanic arc basalts, suggesting an origin within a supra-subduction zone ophiolite sequence. Laser ablation ICP-MS U-Pb zircon dating yields a Neoproterozoic protolith age of 611.7 ±4.7 My, while K-Ar dating of phengite indicates a late Variscan episode (348.1–311.4 Ma), likely reflecting post-metamorphic cooling. The olistostrome material is interpreted as derived from the Fore-Magura Ridge.

Key words: Flysch Carpathians, Magura Nappe, olistostrome, Neoproterozoic metabasite, supra-subduction zone, prasinite, ophiolitic sequence.

INTRODUCTION

Wieser (1952) reported that Książkiewicz had identified a metabasite block in the Pasierbiec Sandstone near the village of Osielec within the Magura Nappe flysch (Fig. 1). He termed it the "ophiolite from Osielec," classifying it as an albite amphibolite or hornblende prasinite (following Angel and Scharizer's classification, *fide* Turner, 1981). He proposed that, based on stratigraphic similarities within the Alpine–Carpathian arc, this ophiolite represents a pre-orogenic eruption, potentially correlative with either Lower Cretaceous Alpine ophiolites or pre-Carboniferous ophiolites in the Central Carpathians (Wieser, 1952). Angel and Scharizer (*fide* Leardi et al., 1986) positioned prasinites between the amphibolite and greenschist facies, possibly equivalent to Escola's (1939) albite-epidote-amphibolite facies. The term "prasinite" typically applies to metamorphosed ophiolites or their derivatives (Leardi et al., 1986).

The presence of metabasites in the Outer Carpathians is enigmatic, as some researchers (e.g., Birkenmajer, 1986; Oszczypko, 1992; Oszczypko et al., 2015) have hypothesized an oceanic crust beneath the Outer Carpathian basins, particularly the Magura Basin.

Detailed geological studies of the Magura Nappe in Osielec, expanded by Cieszkowski et al. (2017), alongside petrological, geochemical, and isotopic investigations (e.g., Anczkiewicz et al., 2016, 2018; Gawęda et al., 2019, 2023), have clarified its context. Initial U-Pb zircon dating has established a 611.7 My age (Anczkiewicz et al., 2016).

* Corresponding author, e-mail: mateusz.szczech@uj.edu.pl

Received: August 9, 2024; accepted: July 26, 2025; first published online: October 20, 2025

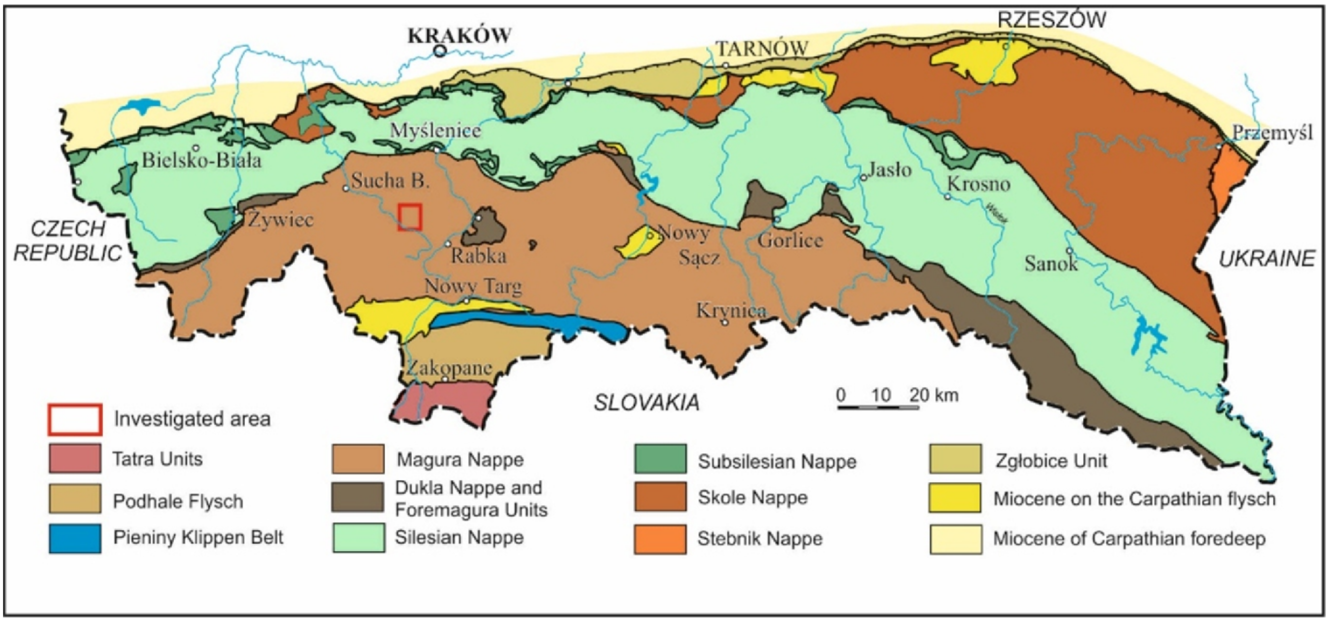

Fig. 1. Geological sketch map of the Polish sector of the Outer Carpathians, showing location of the study area (after Cieszkowski et al., 2017)

This study aims to elucidate the origin and geodynamic context of the Osielec metabasite which is the only known occurrence of this rock type in the Carpathian flysch. Our study offers new insights into its deformation and metamorphic history within the Magura Basin's basement evolution. We focus on the metabasite block's origin and its relationship to the source rocks of the Western Outer Carpathians' flysch units (Cieszkowski et al., 2017), using new geochemical and isotopic data from zircons and micas.

GEOLOGICAL SETTING

The village of Osielec is located in the Western Carpathians (Figs. 1 and 2), on the southern slopes of the Beskid Makowski Mountains along the Skawa River, between Jordanów and Maków Podhalański. Geologically, the Carpathians are divided into the Inner and Outer (Flysch) Carpathians (e.g., Książkiewicz, 1977; Ślączka et al., 2006; Golonka et al., 2019). Flysch sediments were deposited in the deep-sea basins of the Outer Carpathians (e.g., Książkiewicz, 1977; Ślączka et al., 2006; Golonka et al., 2019). The Magura Basin, the innermost of these basins, was bordered to the north by the Grybów (Fore-Magura) Ridge (Książkiewicz, 1962; Ślączka et al., 2006) and to the south-east by the Marmarosh and Magura Ridges (Teťák, 2022). Late Cretaceous to Miocene deposits formed an accretionary prism, which was subsequently detached and folded, resulting in a stack of nappes (Fig. 1).

This study focuses on the Polish sector of the Outer Carpathians, specifically the Magura Nappe, which is subdivided into four facies-tectonic zones (Koszarski et al., 1974). Osielec lies within the Rača and Siary subunits, which represent the northernmost zones of the Outer Carpathians (Cieszkowski et al., 2017). Geological investigations in this area, initiated by Książkiewicz (1966) and others (e.g., Wieser, 1966; Burtan and Szymakowska, 1966; Książkiewicz et al., 1977) and continued by Wójcik and Rączkowski (1994), and Cieszkowski et al. (2017), with recent contributions by Gawęda et al. (2019, 2023), form the foundation of this research.

STRATIGRAPHY

The sedimentary succession of the Rača Subunit in Osielec (Fig. 2) includes the Ropianka Formation (Campanian–Paleocene), Łabowa Shale Formation (uppermost Paleocene–Middle Eocene), Pasierbiec Sandstone Formation (Middle Eocene), Beloveža Formation (Middle–Upper Eocene), and Magura Formation (Upper Eocene–Oligocene; Cieszkowski et al., 2017). The Siary Subunit is represented solely by the Wątkowa Sandstone Member of the Beskid Makowski Formation (Upper Eocene–Oligocene). Traditional lithostratigraphic names (e.g., Książkiewicz, 1966; Wójcik and Rączkowski, 1994; Książkiewicz et al., 2017) are noted in parentheses below.

Ropianka Formation (Inoceramian beds, Ropianka beds): Comprises grey, thin- to medium-bedded, fine- to medium-grained quartz-muscovite sandstones with feldspar and biotite, cemented by siliceous and carbonate materials. These sandstones, commonly parallel-, cross- or convolute-laminated, intercalate with grey or greenish shales.

Łabowa Shale Formation (Paleogene variegated shales): Consists of variegated muddy or clayey shales (predominantly red, subordinately green) with thin-bedded, fine-grained green sandstones.

Pasierbiec Sandstone Formation (Pasierbiec sandstones): Features thick-bedded sandstones, conglomeratic sandstones, conglomerates, and occasional sedimentary breccias, with intercalations of thin shale-sandstone packages. Two sandstone lithotypes coexist (Książkiewicz, 1966; Cieszkowski et al., 2017): the Pasierbiec lithotype (thick- to very thick-bedded, coarse-grained or conglomeratic, with quartz, feldspar, muscovite, glauconite, and lithoclasts of limestone, chert, radiolarite, mudstone, claystone, granitoids, metabasites, amphibolitic and micaceous gneisses, phyllites, and metamorphic schists) and the Osielec lithotype (medium- to thick-bedded, fine- to medium-grained grey to grey-greenish sandstones dominated by quartz with feldspar, muscovite, and glauconite). Palaeocurrent data indicate a northern sediment source. Olistostromes within this formation include debrites with shaley clasts, pebbles, boulders, and exotic blocks, including metabasites (0.5–3.5 m across), first described as ophiolites by Wieser (1952).

Beloveža Formation (Beloveža beds, Hieroglyphic beds): Dominated by grey-greenish, thin-bedded, fine-grained, parallel-laminated sandstones interbedded with grey-greenish shales, composed mainly of quartz with minor feldspar, glauconite and muscovite. Thick-bedded Pasierbiec-type sandstones occur in the lower part.

Magura Formation (Magura beds): Consists of thick-bedded, massive, grey (bluish when fresh), medium- to coarse-grained muscovite sandstones, predominantly quartz with feldspar, muscovite, chlorite, and lithoclasts of mica schist, igneous rocks, and quartzite, occasionally interbedded with shales. Palaeocurrents suggest derivation from the southeast and east-southeast.

Wątkowa Sandstone Member (Magura glauconitic sandstones): Similar to the Magura Formation but rich in glauconite, with detrital material sourced from the north and north-east (Cieszkowski et al., 2017).

TECTONICS

The study area lies within the Rača and Siary subunits of the Magura Nappe. Książkiewicz (1966) identified the "Osielec Skiba" tectonic unit (a complex thrust sheet), which Cieszkowski et al. (2017) subdivided into the southern Bystra Thrust Sheet and the northern Osielczyk Thrust Sheet (Fig. 2). The Osielczyk Thrust Sheet features the northwards-overturned Grzybówka Anticline, hosting the Pasierbiec Sandstone Formation with ophiolitic blocks, and thrust over the Wątkowa Sandstone Member. Its southern limb includes the irregular Wronków Syncline. Northwest of Głodkówka hamlet, a local anticline of Pasierbiec Sandstone occurs. The Bystra Thrust Sheet overrides the Osielczyk Thrust Sheet from the south, with the Głodkówka Anticline (Ropianka and Łabowa Shale formations in the core, Beloveža Formation in the southern limb) transitioning southwards into the Łysa Mount Syncline (Magura Formation sandstones). Fold structures and thrust sheets are intersected by a transverse fault system oriented N–S, NNW–SSE, NNE–SSW, NW–SE, and NE–SW.

METHODS

Field investigations by Cieszkowski et al. (2010) involved collecting 7 metabasite samples from an olistostrome block (2.5 2.0 m) in the Osielczyk Stream valley (Fig. 3). Twenty thin sections were prepared, cut in the XZ plane of the strain ellipsoid (parallel to lineation, perpendicular to foliation) to observe structural features and porphyroclasts (Passchier and Trouw, 2005).

Microstructural observations and standardless chemical analyses were conducted at the Laboratory of Field Emission Scanning Electron Microscopy and Microanalysis, Institute of Geological Sciences, Jagiellonian University, using a *JEOL 5410* microscope with a *Voyager 3100 (NORAN) EDS* spectrometer and a *HITACHI S-4700* microscope with a *Vantage (NORAN) EDS* spectrometer (100 s analysis time, 20 kV acceleration voltage, ZAF correction via Proza Phi-Rho-Z algorithm).

Whole-rock analyses of 4 samples were performed at Bureau Veritas Commodities Canada Ltd. Mineral Laboratories. Major oxides and trace elements were analyzed by ICP-emission spectrometry after lithium metaborate/tetraborate fusion and dilute nitric acid digestion. Loss on ignition (LOI) was determined by weight difference after ignition at 1000°C for >2 hours. Rare earth elements (REEs) were analyzed by ICP-MS following the same fusion and digestion process. Precious and base metals were digested in aqua regia and analysed by ICP-MS.

Laser ablation ICP-MS U-Pb zircon dating was conducted at the Institute of Geological Sciences, Polish Academy of Sciences, Kraków Research Centre, following Anczkiewicz and Anczkiewicz (2016). Zircons were separated via crushing, sieving, heavy liquid, and magnetic separation, with final purification by hand-picking under a stereomicroscope. Zircons were mounted in epoxy, polished, and imaged via cathodoluminescence (CL) using SEM at AGH University of Kraków. Data reduction used Iolite v. 3 (Paton et al., 2010, 2011), with concordia diagrams and age calculations performed in Isoplot v. 4.15 (Ludwig, 2008). Zircon Z91500 (Wiedenbeck et al., 1995) served as the primary standard, with GJ-1 (Jackson et al., 2004) and Plešovice (Sláma et al., 2008) as secondary standards (accurate within < 0.6% precision).

K-Ar dating of phengite from S-C structures (Figs. 4 and 5B) was conducted on 3 samples at the ClayLab, Institute of Geological Sciences, Polish Academy of Sciences. Two portions per sample were analysed for potassium using a *Sherwood Model 420* flame photometer, and a third for argon using a Nu Instruments Noblesse multicollector noble-gas spectrometer (NG039). Samples were melted with a 972 nm infrared laser, evacuated to ~10^{-10} mbar, and cleaned via titanium sublimation and getter pumps (Z-100, SAES Getters). The ^{38}Ar spike was calibrated with the GL-O standard (Odin, 1982), measured thrice per batch of 5 samples. Daily air sample aliquots were corrected $^{40}Ar/^{36}Ar$ and $^{40}Ar/^{38}Ar$ ratios for mass fractionation and detector efficiencies (Lee et al., 2006). Age errors incorporated uncertainties from spectrometry, weighing, potassium measurements, spike normalization, and air aliquot ratios.

RESULTS

PETROGRAPHIC DESCRIPTION

The metabasites are massive, variably coloured (pale to dark green) rocks (Figs. 3, 4 and 5A). They are strongly deformed, with distinct color-zoned domains cut by veinlets (Fig. 4). Dark green zones are massive, while pale green zones show foliation.

Plagioclase (albite) and amphibole (Mg-hornblende) are the main metamorphic minerals, likely formed under amphibolite facies conditions, occurring as porphyroclasts (augens) deformed by later ductile and brittle processes. The result of ductile deformation is clearly visible as foliation. The rock was also deformed in brittle conditions, as shown by numerous fractures and fragmentation of plagioclases. Quartz shows specific optical properties such as undulose extinction, related to brittle-ductile deformation (Cieszkowski et al., 2010; Anczkiewicz et al., 2016). Albite ($Ab_{99–91}$, Table 1) porphyroclasts in foliated zones display albite-law twinning and saussuritic aggregates (zoisite/epidote) in their cores, commonly fractured and displaced, surrounded by flakes of secondary phengite forming foliation planes (Fig. 5B). Phengite classification ($Si/Al^{IV} > 3$, Table 2) follows Deer et al. (1962). Amphiboles (Table 3), classified per Leake et al. (1997) as calcic (Ca^{A} 1.50; (Na+K)? < 0.50), include Mg-hornblende (mg# = 0.55–0.65) with strong pleochroism (yellow green to olive-green) in massive zones, partially replaced by actinolite (mg# = 0.66–0.69), epidote, sphene, chlorite, Mg-calcite and opaque minerals (Fig. 5C).

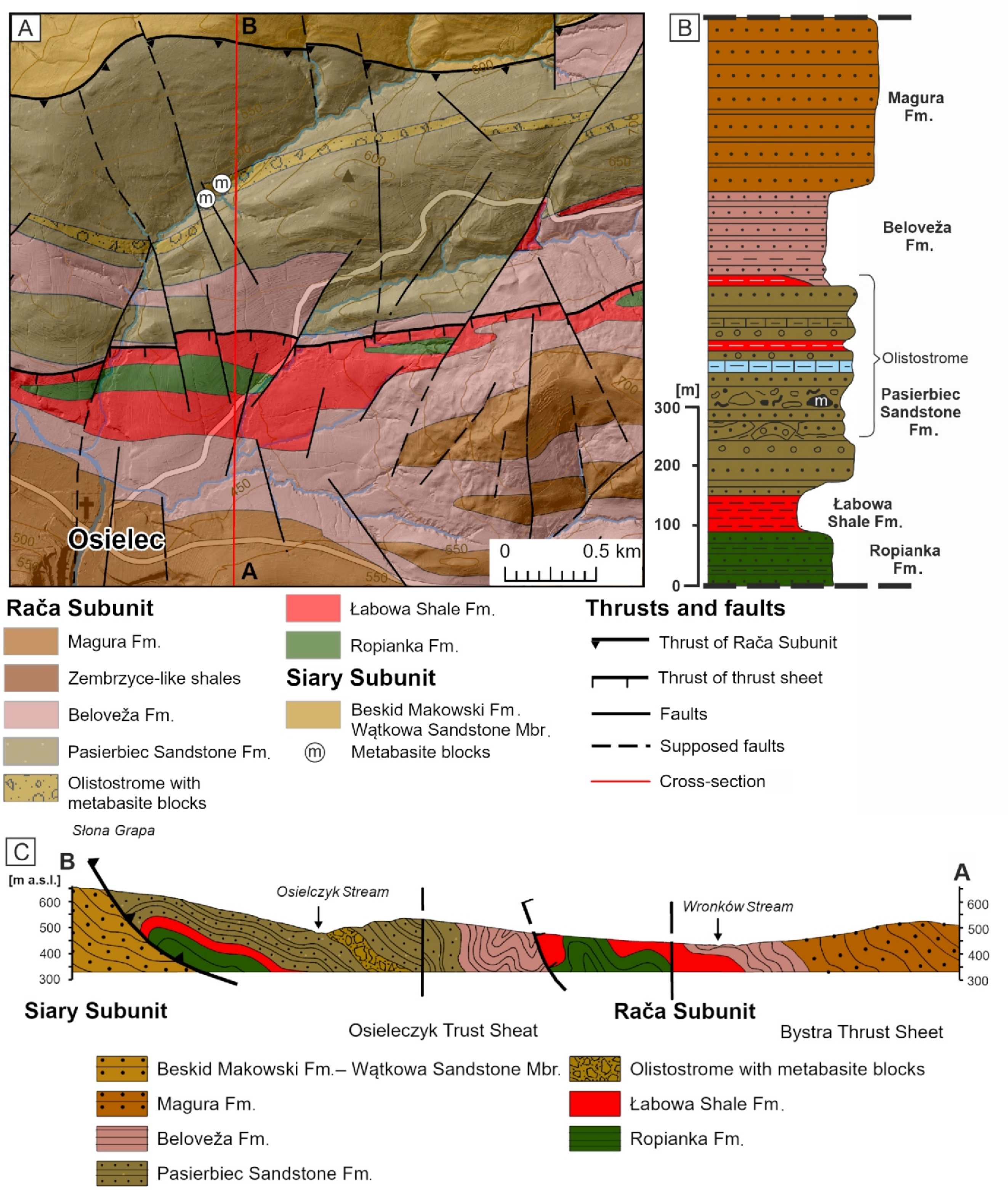

Fig. 2. Location of metabasite blocks in the Osielec area (after Cieszkowski et al., 2017, significantly modified)

A – geological map of Osielec; **B** – lithostratigraphic log of the sedimentary succession of the Magura Nappe in Osielec; **C** – geological cross-section

Fig. 3. Metabasite

A – block of metabasite exposed in Osielczyk Stream with Prof. M. Cieszkowski; **B** – block of metabasite exposed in Osielczyk Stream

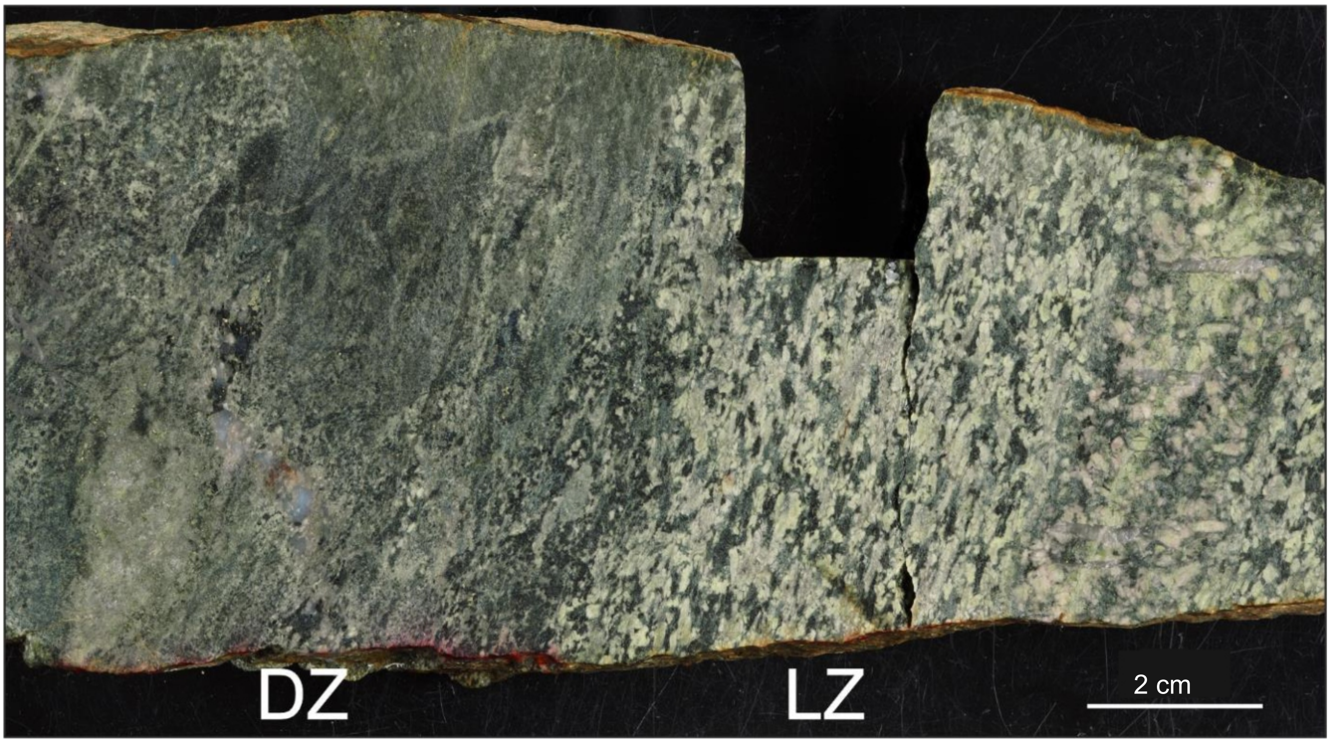

Fig. 4. Hand specimen chipped from the metabasite block with two zones

DZ – dark massive zone, LZ – light foliated zone. Section in the XZ plane of the strain ellipsoid (perpendicular to the foliation, parallel to the lineation)

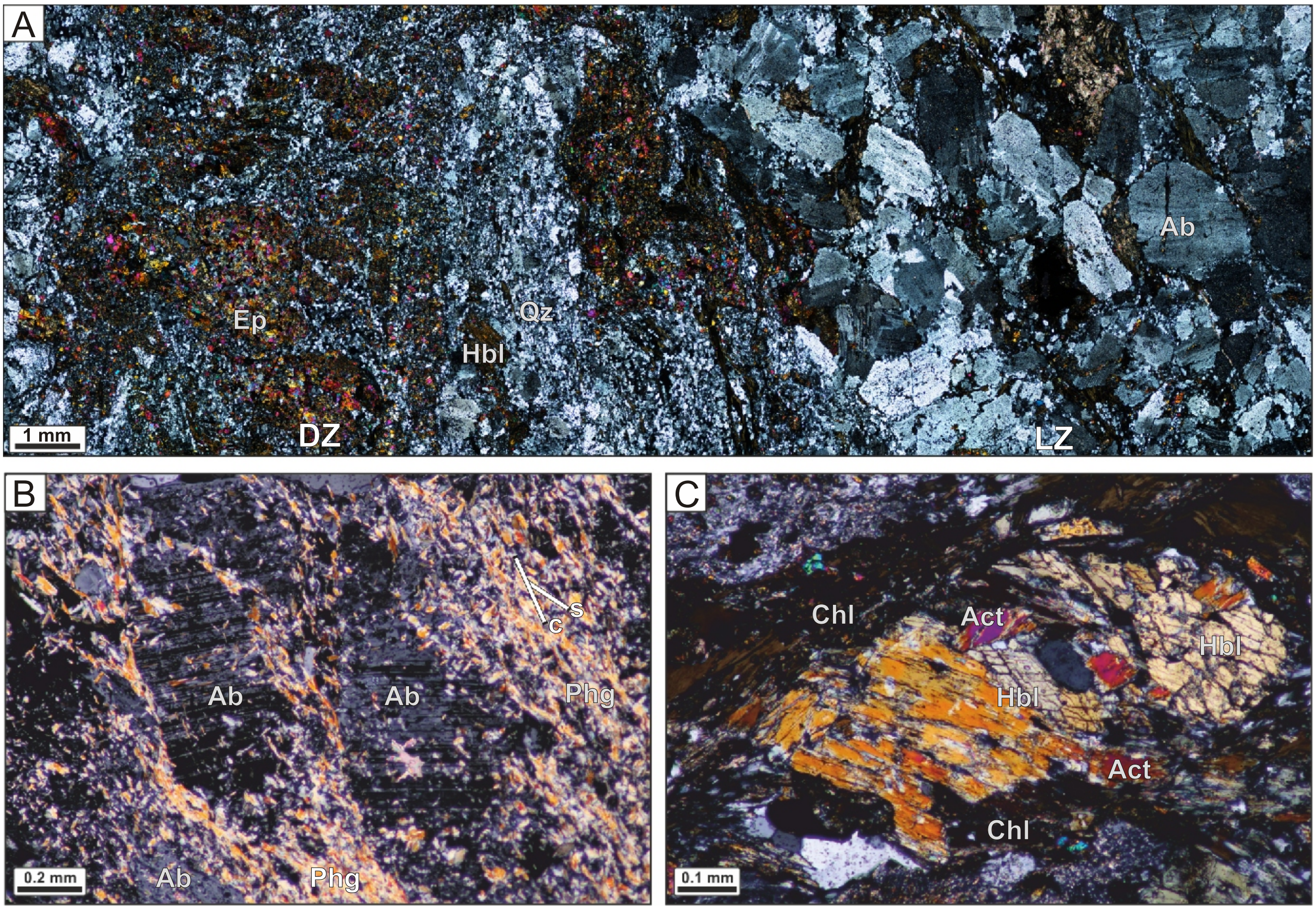

Fig. 5. Microphotographs

A – general overview of a OGK4 sample thin section with crossed polars: DZ – dark massive zone, LZ – light foliated zone; **B** – albite porphyroclasts (augens) surrounded by foliation marked by the orientation of white mica flakes (sample no. OGK 8-1). Crossed polars; **C** – an asymmetrical Mg-hornblende porphyroclast surrounded by chlorite flakes (sample no. OGK 5). Crossed polars. Mineral abbreviations: Ab – albite, Act – actinolite, Chl – chlorite, Ep – epidote, Hbl – hornblende, Phg – phengite

The rocks are crosscut by calcite and quartz veinlets. Phengite (pale green zones) and chlorite (dark green zones) define the fabric of the rock (Fig. 5). Accessory minerals include apatite, ilmenite and rare zircon.

GEOCHEMICAL FEATURES

Whole-rock analyses (Table 4) indicate moderate SiO_2 (55.1–57.8 wt.%), Fe_2O_3 (up to 7.91 wt.%), and TiO_2 (up to 1.03 wt.%) contents, with enrichments in Al_2O_3 (up to 18.56 wt.%) and Na_2O (up to 5.44 wt.%). LOI (3.2–5.5 wt.%) reflects hydrous minerals (amphiboles, chlorites, micas). The Mg number (37–39%) is low. Compatible elements (Cr, Ni, Co, V) show low to moderate enrichment, while HFSEs (Zr, Hf, Th, U) and LILEs (Sr, Ba, K, Rb) are depleted. Total REE (ÓREE = 92.3–95.5 ppm) is low.

Chondrite-normalized trace element patterns (Fig. 6A) reveal depletions in LILEs (Ba, Sr) and HFSEs (Ta, Nb, P, Ti) and positive anomalies in LILEs (Rb, K) and HFSEs (U, Hf, Zr, La, Ce, Nd). REE patterns (Fig. 6B) show a slightly negative Eu anomaly (Eu/Eu* = 0.83–0.91) and flat LREE/HREE fractionation ($(La/Yb)_n$ = 5.9–5.6), typical of mixed basaltic series (Miyashiro and Shido, 1975). Moderate fractionation occurs in LREE vs. HREE ($(La/Sm)_n$ = 2.4–2.3) and MREE vs. HREE ($(Tb/Yb)_n$ = 1.3–1.2). N-MORB-normalized patterns confirm positive Rb, Ba, K, La, Hf, Zr anomalies and negative Ta, Nb, Sr, P, Ti anomalies.

The geochemical signature (low SiO_2, high FeO_t, MgO, transition elements, TiO_2, P_2O_5) suggests a mafic origin, with high Al_2O_3 indicating affinity to high-alumina basalts (HAB) from island arcs (Tilley, 1950; Kuno, 1960; Koszowska et al., 2007).

The phengite composition allowed calculation of the pressure peak according to the formula given by Kamzolkin et al. (2016). Based on the presence of albite, zoisite and actinolite, as well as the dynamic recrystallization of quartz, a temperature of 300°C was inferred. This allows estimation of pressure at 12.5 kbar for the OGK-1 sample and 12.3 kbar for the OGK-2 sample.

GEOCHRONOLOGY

Despite zircon's rarity in metabasites, 38 crystals were analysed via LA-ICP-MS U-Pb dating (Fig. 7 and Table 5). CL imaging shows simple oscillatory zoning without post-crystallization modification (Fig. 7B). Analyses yield a concordant age of 611.7 ±4.7 Ma (Fig. 7A), interpreted as the protolith's magmatic crystallization age.

K-Ar dating of phengite from S-C structures (Table 6) spans from 348.1 ±9.5 to 311.4 ±9.8 Ma, reflecting metamorphism and cooling during the middle to late Variscan orogeny, followed by shearing and deformation.

Table 1

Examples of chemical analyses (EDS method) of albite

	Sample OGK7 Analysis no. 4a (1) Albite phenocryst	Sample OGK1A/1 Analysis no. 7a/3 Albite phenocryst	Sample OGK8/2 Analysis no. 7a/1 Albite phenocryst
	Wt.%		
SiO_2	68.98	69.41	68.84
Al_2O_3	18.61	18.66	19.68
Fe_2O_3*	0.06	0.08	0.09
MnO	0.00	0.08	0.00
CaO	0.23	0.14	1.01
SrO	0.70	0.59	0.24
BaO	0.19	0.07	0.05
Na_2O	10.55	10.96	10.09
K_2O	0.67	0.01	0.00
Sum	100.00	100.00	100.00
	Number of cations calculated on 8 at. O**		
Si	3.027	3.033	3.000
Al	0.963	0.961	1.011
Fe	0.002	0.003	0.003
Mn	0.000	0.020	0.000
Ca	0.011	0.035	0.047
Sr	0.018	0.015	0.006
Ba	0.003	0.001	0.001
Na	0.898	0.929	0.853
K	0.037	0.001	0.000
Sum	4.959	4.951	4.920
Ab	94.9 %	99.3 %	94.8%
An	1.1 %	0.7 %	5.2%
Or	3.9 %	0.1 %	0.0%
Sum	99.9 %	100.1 %	100.0%

* – all Fe are calculated as Fe^{3+} as proposed by Deer et al. (2001); endmembers (Ab, An and Or) are calculated:
Ab = 100(Na/Na+Ca+K), An = 100(Ca/Na+Ca+K) and
Or=100(K/Na+Ca+K) (according to Deer et al., 2001)

Table 2

Examples of chemical analyses (EDS method) of white micas

	Sample OGK1b analysis no.2-4e(1) phengite in S-C structure	Sample OGK1b Analysis no.2-4c(1) phengite in S-C structure
	Wt.%	
SiO_2	53.20	53.29
TiO_2	0.00	0.45
Al_2O_3	26.47	26.99
V_2O_5	0.43	0.00
$Fe_2O_3^*$	3.40	3.32
MnO	0.16	0.00
MgO	4.39	3.89
CaO	0.46	0.11
Na_2O	0.39	0.63
K_2O	11.05	11.24
Cl	0.02	0.08
Sum	100.00	100.00
	Number of cations calculated on 22 at. O**	
Si	6.79	6.80
Al^{IV}	1.21	1.20
Si+ Al^{IV}	8.00	8.00
Al^{VI}	2.77	2.86
Ti	0.00	0.04
V	0.04	0.00
Fe^{3+}	0.33	0.32
Mn	0.02	0.00
Mg	0.84	0.74
Al^{VI}+Ti+V+Fe^{3+}+Mg	3.99	3.96
Ca	0.06	0.02
Na	0.10	0.16
K	1.80	1.83
Ca+Na+K	1.96	2.00
Cl	0.06	0.02
mg	0.72	0.70

* – all Fe are calculated as Fe^{3+} as proposed by Holland and Blundy (1994); ** – after Robinson et al., (1982) the cations number are calculated on 22 oxygen atoms because did not determine the water content in the micas

Table 3

Examples of chemical analyses (EDS method) of amphiboles (Mg-hornblende and secondary actinolite)

	Sample OG-1b/2 Analysis no. 8b (1) Actinolite (rim)	Sample OG-1b/2 Analysis no. 8a (1) Mg-hornblende (central part)
	wt.%	
SiO_2	50.08	56.15
TiO_2	0.60	0.25
Al_2O_3	5.82	1.34
V_2O_5	0.09	0.06
FeO*	16.51	12.66
MgO	12.28	15.67
MnO	0.58	0.64
CaO	12.68	12.60
Na_2O	0.84	0.48
K_2O	0.46	0.06
Cl	0.07	0.08
Sum	100.00	100.00
	Number of cations calculated on 23 at. O**	
Si	7.25	7.89
Al^{IV}	0.75	0.11
Si+Al^{IV}	8.000	8.00
Al^{VI}	0.25	0.11
V	0.01	0.01
Ti	0.07	0.03
Fe	2.00	1.49
Mn	0.07	0.08
Mg	2.65	3.28
Al^{VI}+V+Ti+Fe+Mn+Mg	5.04	4.993
Ca	1.97	1.90
Na	0.24	0.13
K	0.08	0.01
Ca+Na+K	2.29	2.04
Cl	0.02	0.02
mg=Mg/Mg+Fe	0.6	0.70
Mg:Fe	1.3	2.2
Na+K	0.32	0.14

* – all Fe are calculated as Fe^{2+} as proposed by Holland and Blundy (1994); ** – after Robinson et al., (1982) the cations number are calculated on the basis 23 oxygen atoms because we did not determine the water content in the amphibole studied

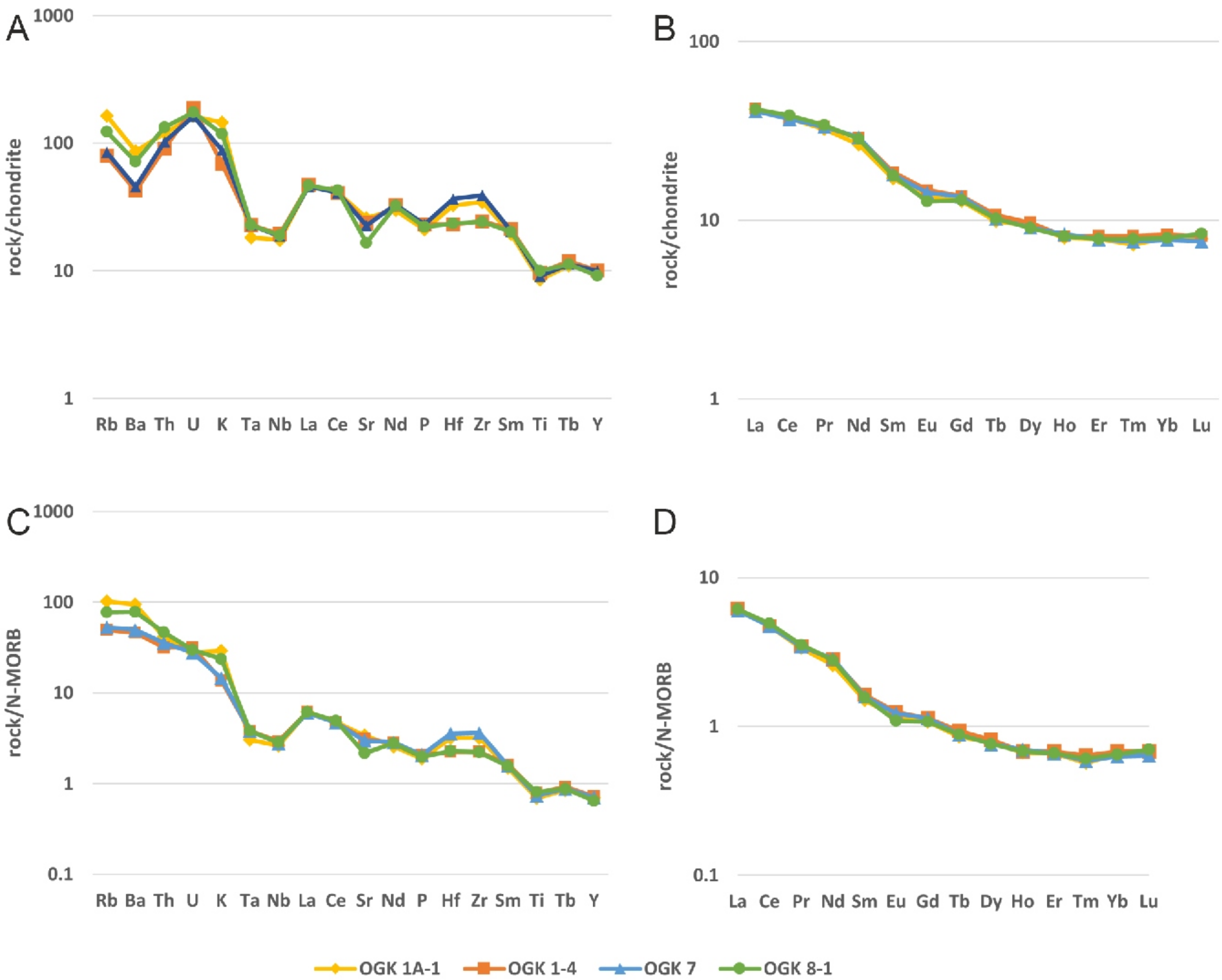

Fig. 6. Element normalization patterns for the metabasite studied

A – spider diagrams of trace elements to chondrite normalization; **B** – spider diagrams of REEs to chondrite normalization; **C** – spider diagrams of trace elements to N-MORB normalization; **D** – spider diagrams of REEs to N-MORB normalization. Chondrite normalizations after Taylor and McLennan (1985), N-MORB normalizations after Sun and McDonough (1989)

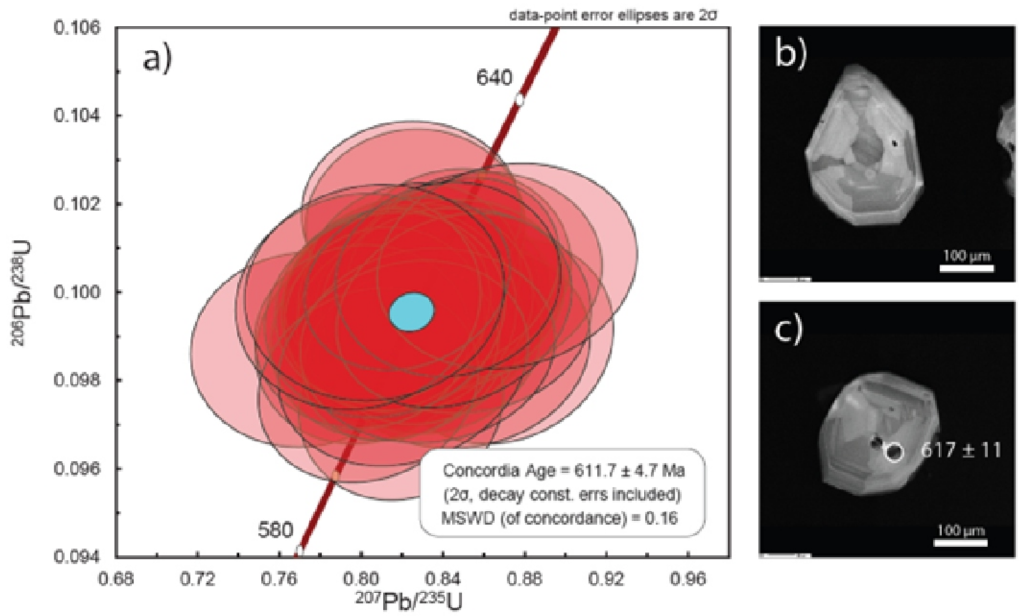

Fig. 7. Laser ablation ICP-MS U-Pb zircon dating results

A – Concordia plot; **B, C** – (CL) images of selected zircon crystals demonstrating simple oscillatory zoning. Apparent age indicated in the analysed spot is ^{206}Pb-^{238}U (C)

Table 4

Chemical composition of the rocks studied

	OGK 1A-1	OGK 1-4	OGK 7	OGK 8-1
wt.%				
SiO_2	55.90	55.12	55.31	57.80
TiO_2	0.88	1.00	0.94	1.03
Al_2O_3	17.37	18.56	17.78	17.49
Fe_2O_3*	7.71	7.80	7.91	7.06
MnO	0.12	0.12	0.13	0.13
MgO	4.23	4.47	4.57	3.80
CaO	5.21	3.88	3.84	2.53
Na_2O	3.60	5.44	5.15	3.90
K_2O	2.10	0.99	1.05	1.71
P_2O_5	0.22	0.24	0.24	0.23
LOI	3.60	3.60	3.20	5.50
Total	100.94	101.26	100.12	101.18
ppm				
Ba	597	291	313	495
Co	20.8	21.9	22.8	23.5
Cs	3.0	1.1	1.4	1.9
Cr	70	48	48	82
Ga	19.1	16.4	18.0	17.9
Hf	6.5	4.6	7.3	4.7
Nb	6.1	6.8	6.5	6.6
Ni	25.2	23.4	20.3	30.9
Rb	57.4	27.8	29.6	43.1
Sc	57.4	27.8	29.6	43.1
Sr	305.4	279.1	266.7	195.0
Ta	0.4	0.5	0.5	0.5
Th	5.0	3.8	4.3	5.6
U	1.3	1.5	1.3	1.4
V	139	131	135	166
W	0.6	0.7	0.7	0.6
Zr	236.3	166.3	267.1	164.6
Mo	0.1	<0,1	<0,1	0.1
Cu	11.6	28.0	21.6	91.8
Pb	1.5	1.9	2.1	1.8
Zn	66	98	87	80
As	6.2	3.0	3.1	4.5
Y	19.7	20.2	19.9	18.3
La	15.3	15.4	15.0	15.3
Ce	35.5	35.3	35.3	36.8
Pr	4.43	4.57	4.55	4.66
Nd	18.8	20.5	20.8	20.3
Sm	3.94	4.29	4.15	4.11
Eu	1.17	1.28	1.24	1.11
Gd	3.92	4.17	4.15	3.95
Tb	0.57	0.62	0.59	0.59
Dy	3.54	3.70	3.47	3.45
Ho	0.68	0.69	0.71	0.69
Er	1.95	2.03	1.95	1.96
Tm	0.26	0.29	0.27	0.28
Yb	1.98	2.06	1.93	1.97
Lu	0.30	0.31	0.29	0.32
ΣREE	92.3	95.2	94.4	95.5
Mg#	0.38	0.39	0.39	0.37
Eu/Eu*	0.90	0.91	0.90	0.83
$(La/Yb)_N$	5.83	5.63	5.86	5.86

Total iron as Fe_2O_3; LOI – loss on ignition

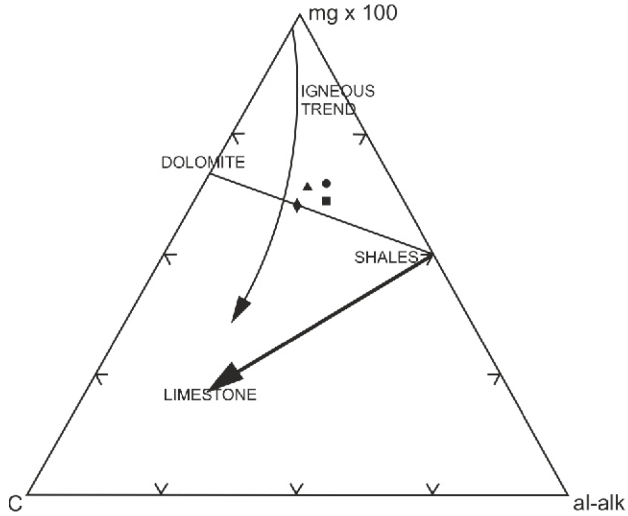

Fig. 8. The position of the metabasite studied on diagram after Leake (1964)

Symbols as for Figure 6

DISCUSSION

PETROLOGICAL AND GEOCHEMICAL IMPLICATIONS

Primary minerals include albite porphyroclasts (with saussuritic zoisite/epidote cores) and Mg-hornblende porphyroclasts, partially replaced by actinolite, epidote, sphene, chlorite, Mg-calcite and opaques. Foliation, marked by phengite and chlorite, indicates shearing and metamorphism (Passchier and Trouw, 2005; Smulikowski et al., 2011). Gawęda et al. (2019) identified two assemblages in similar Osielec mafic clasts: (1) actinolitic hornblende–actinolite–epidote–biotite–titanite–albite-oligoclase–chlorite–rutile, and (2) chlorite–quartz–epidote–sericite tied to foliation. Both quartz and plagioclases show evidence of deformation; however, due to different rheological properties, this deformation is brittle in plagioclases, whilst quartz underwent dynamic recrystallization (Fig. 5A).

Geochemically, the metabasites exhibit moderate Fe_2O_3 and TiO_2, low to moderate transition metals, and depleted HFSEs and LILEs, with positive Zr and Hf anomalies linked to zircon presence. Niggli's (1948) parameters (Fig. 8) corroborate a magmatic protolith. Immobile element ratios (Zr/Ti vs. Nb/Y; Fig. 9) classify the protolith as basaltic andesite or andesite, with mixed arc calc-alkaline/tholeiitic signatures (V vs. FeO_t/MgO; Fig. 10). Diagrams (Figs. 11–13) place the metabasites in arc basalt fields, suggesting a subduction setting. Positive Rb, Ba, K anomalies may reflect sediment contamination, while abundant zircon (Zr, Hf anomalies) indicates a hybrid magma distinct from typical ophiolites. Gawęda et al. (2019) suggest the protholith had a mid-ocean ridge (MOR) character. In our opinion, the geochemical signature shows a rather mixed calc-alkaline/tholeiitic provenence. In their 2023 paper, Gawęda et al. (2019) proposed an arc setting with crustal contamination for the protolith, which is more consistent with our results.

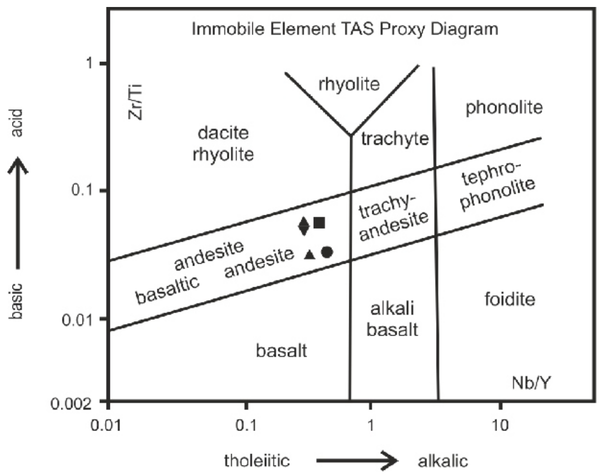

Fig. 9. The plot of the metabasites studied on a Zr/Ti vs Nb/Y diagram based on immobile elements (after Floyd and Winchester, 1975 and modified by Pearce, 1996)

Symbols as for Figura 6

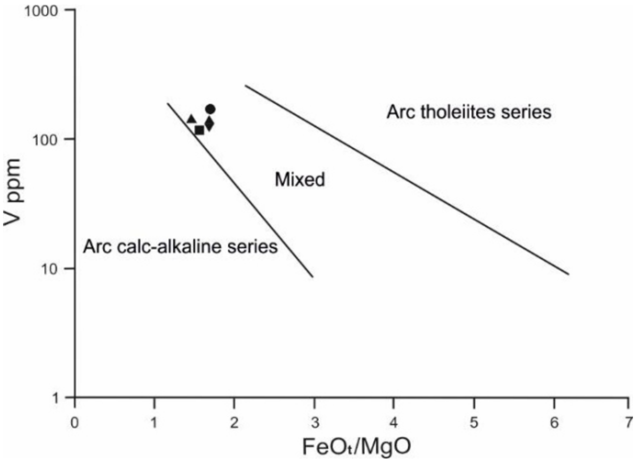

Fig. 10. The position of the metabasite studied on a V–FeO$_t$/MgO diagram (after Miyashiro and Shido, 1975)

Symbols as for Figure 6

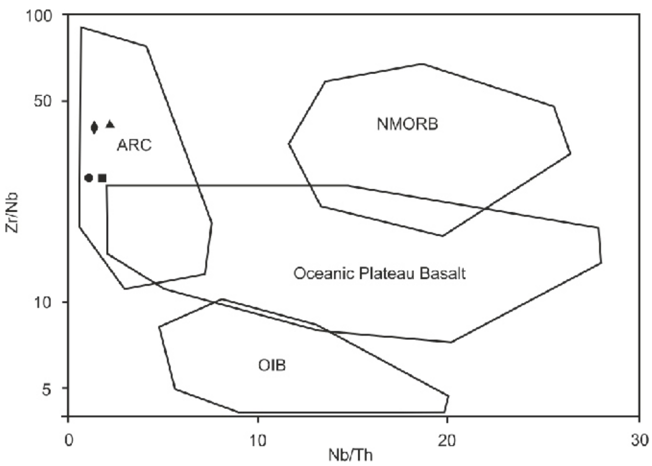

Fig. 11. The position of the metabasites studied on a Zr/Nb–Nb/Th diagram (after Condie, 2005)

Symbols as for Figure 6

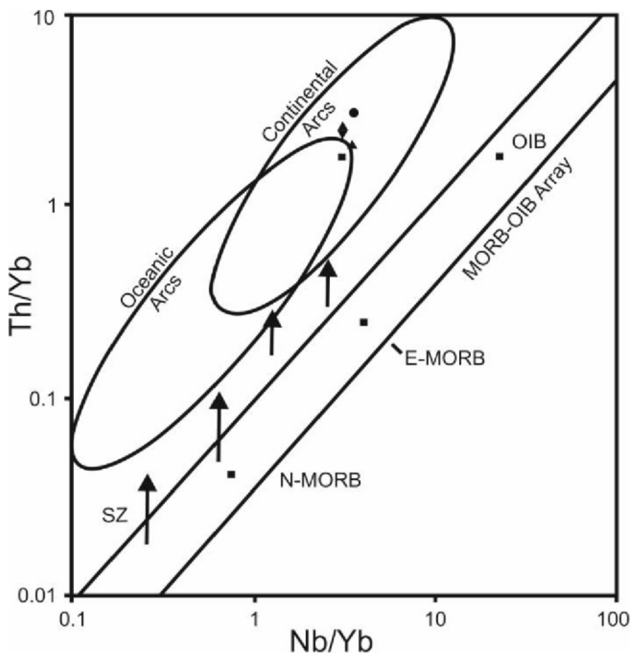

Fig. 12. The position of the metabasite studied on a Th/Yb–Nb/Yb diagram (after Pearce, 1983; N-MORB and E-MORB values from Sun and McDonough, 1989)

Symbols as for Figure 6; the arrows mark the hybridization process of the original magma

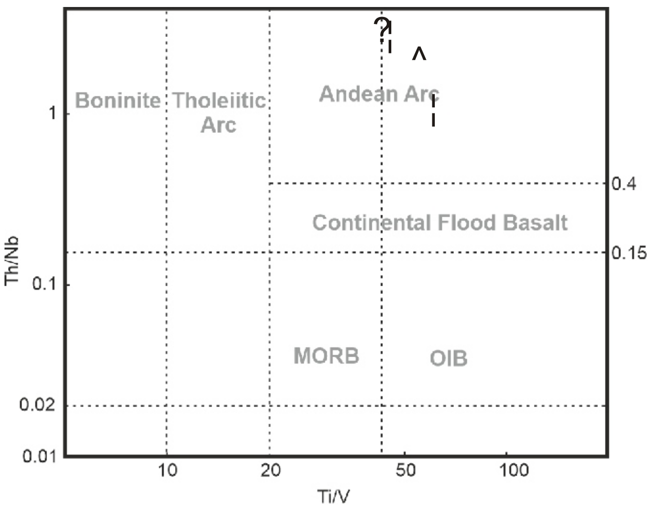

Fig. 13. The position of the metabasite studied on a Th/Nb–Ti/V diagram (after Shervais, 2021)

Symbols as for Figure 6

Table 5

Summary of laser ablation ICP-MS U-Pb zircon dating

	Isotopic ratios							Apparent age (My)					
Zircon #	$^{207}Pb/^{235}U$	2SE	$^{206}Pb/^{238}U$	2SE	$^{207}Pb/^{206}Pb$	2SE	Rho	$^{207}Pb/^{235}U$	2SE	$^{206}Pb/^{238}U$	2SE	$^{207}Pb/^{206}Pb$	2SE
Z - 2	0.869	0.045	0.0989	0.0019	0.0636	0.0032	0.12	629	24	607.7	11.0	651	110
Z - 3	0.828	0.049	0.0998	0.0017	0.0603	0.0035	0.12	602	27	613.2	10.0	480	120
Z - 4	0.830	0.052	0.0994	0.0020	0.0601	0.0034	0.24	601	29	610.6	12.0	480	120
Z - 5	0.849	0.052	0.0988	0.0019	0.0627	0.0038	0.07	613	28	607.0	11.0	570	120
Z - 7	0.772	0.045	0.0987	0.0018	0.0574	0.0033	0.04	574	25	607.5	11.0	390	110
Z - 10	0.820	0.042	0.0992	0.0017	0.0601	0.0029	0.13	597	24	609.5	9.9	493	110
Z - 11	0.812	0.041	0.0998	0.0017	0.0592	0.0029	0.13	595	23	613.0	10.0	473	100
Z - 12	0.804	0.045	0.0989	0.0019	0.059	0.0032	0.13	596	26	607.8	11.0	480	120
Z - 14	0.835	0.044	0.0990	0.0018	0.0612	0.0031	0.09	607	25	608.5	10.0	527	110
Z - 15	0.820	0.041	0.0975	0.0018	0.0611	0.0029	0.09	600	23	599.5	10.0	553	100
Z - 16	0.815	0.048	0.0990	0.0019	0.0596	0.0034	0.09	593	28	608.5	11.0	470	120
Z - 17	0.830	0.041	0.0991	0.0017	0.0613	0.0029	0.09	610	23	609.0	9.9	581	99
Z - 18	0.827	0.044	0.1015	0.0018	0.059	0.003	0.02	605	24	623.1	10.0	470	110
Z - 19	0.819	0.046	0.1001	0.0017	0.0589	0.0031	0.17	593	26	614.5	10.0	430	110
Z - 20	0.848	0.045	0.1006	0.0018	0.0613	0.0032	0.04	614	25	617.7	11.0	550	110
Z - 21	0.825	0.044	0.1018	0.0017	0.0594	0.0031	0.01	602	25	624.5	10.0	450	110
Z - 24	0.826	0.043	0.1004	0.0017	0.0595	0.0029	0.07	604	24	616.3	9.9	508	100
Z - 26	0.839	0.050	0.0999	0.0018	0.061	0.0034	0.14	609	28	613.4	11.0	540	120
Z - 27	0.827	0.047	0.0998	0.0018	0.0604	0.0034	0.06	605	26	613.2	11.0	500	120
Z - 28	0.856	0.051	0.1004	0.0019	0.0632	0.0039	0.09	627	30	616.6	11.0	600	130
Z - 29	0.818	0.040	0.0993	0.0016	0.0599	0.0028	0.02	600	22	610.4	9.4	519	100
Z - 32	0.819	0.047	0.0996	0.0019	0.0597	0.0034	0.03	598	27	611.8	11.0	470	120
Z - 34	0.845	0.043	0.1004	0.0018	0.061	0.0028	0.20	614	24	616.6	10.0	553	100
Z - 35	0.847	0.054	0.0996	0.0019	0.0617	0.0039	0.00	605	30	611.5	11.0	500	130
Z - 36	0.820	0.039	0.0986	0.0016	0.0601	0.0027	0.20	605	22	606.3	9.4	546	91
Z - 39	0.812	0.040	0.0994	0.0017	0.0593	0.0028	0.04	599	23	610.9	9.7	493	98
Z - 40	0.801	0.043	0.0990	0.0017	0.0587	0.0031	0.04	587	24	608.3	9.8	440	110
Z - 41	0.811	0.043	0.0997	0.0018	0.0594	0.003	0.10	595	25	612.6	10.0	490	110
Z - 42	0.804	0.044	0.0979	0.0018	0.0598	0.0031	0.15	596	25	601.8	10.0	530	110
Z - 43	0.833	0.051	0.0988	0.0018	0.0608	0.0036	0.07	600	29	607.9	11.0	500	130
Z - 45	0.812	0.048	0.0995	0.0019	0.0598	0.0035	0.12	596	28	611.0	11.0	480	130
Z - 46	0.821	0.050	0.0984	0.0019	0.0615	0.0036	0.18	600	28	605.1	11.0	530	120
Z - 47	0.846	0.047	0.0996	0.0018	0.0626	0.0033	0.20	611	27	612.1	11.0	560	120
Z - 49	0.799	0.049	0.0998	0.0020	0.0582	0.0035	0.08	584	28	612.9	12.0	410	130
Z - 50	0.872	0.052	0.1006	0.0019	0.0631	0.0037	0.12	628	29	617.5	11.0	600	130
Z - 51	0.823	0.041	0.1002	0.0016	0.0595	0.0028	0.19	603	23	615.3	9.7	508	100
Z - 52	0.843	0.045	0.1003	0.0018	0.0615	0.0033	0.06	616	26	616.2	11.0	550	110
Z - 54	0.807	0.052	0.1000	0.0020	0.0578	0.0035	0.06	587	29	614.4	12.0	420	130

Table 6

Results of K-Ar dating measurements

Sample	% K_2O	Mass [mg]	% $^{40}Ar^*$	Age [My]	2σ error [My]	Age total [My]	2σ error total [My]
OG-1b	1.8953	30.58	86.0	322.53	11.41	325.9	11.9
			42.1	3.40	0.47		
OG-3	1.8032	26.28	88.2	345.97	9.14	348.1	9.5
			29.5	2.16	0.33		
OG-6	1.6765	20.66	84.2	310.24	8.42	311.4	9.8
			9.8	1.20	1.35		

GEOCHRONOLOGICAL AND PALAEOGEOGRAPHICAL IMPLICATIONS

The Outer Carpathians' flysch deposits sourced material from surrounding ridges which separated sedimentary basins of the Outer Carpathians (Ślączka et al., 2006; Golonka et al., 2019). Ophiolite-derived detritus (e.g., chromium spinels) in the Magura Unit (Oszczypko and Salata, 2005; Bónová et al., 2017) suggests that the material was derived from the Marmarosh Massif, which was bordering the Magura Basin from the SE (Ślączka et al., 2006; Teťák, 2022). On the other hand, Osielec olistoliths occur within the Pasierbiec Sandstone Formation, the clastic material of which was transported from the Fore-Magura Ridge located to the north (Cieszkowski et al., 2017; Waśkowska et al., 2025).

This formation represents Middle Eocene submarine fans and submarine mass-transport systems in the Magura Basin's Rača subbasin (Cieszkowski et al., 2017; Teťák, 2022). Palaeocurrents indicate derivation from the north, from the Grybów (Fore-Magura) Ridge, activated tectonically during this period unlike adjacent basins (Książkiewicz, 1962; Ślączka et al., 2006).

The Outer Carpathian basement comprises the Brunovistulicum and Małopolska Massif, between the Variscan Bohemian Massif and Precambrian East European Craton (Dudek, 1980; Żelaźniewicz et al., 2009, 2011). Gawęda et al. (2019, 2023) suggested an oceanic floor origin from the Paleo-Asian Ocean, while the lack of zircon overgrowths (Finger et al., 1999) and stratigraphic context tie the olistoliths to the Fore-Magura Ridge, possibly linked to Brunovistulicum. The 611.7 ±4.7 Ma U-Pb age aligns with U-Pb apatite cooling ages (614 ±3 Ma; Gawęda et al., 2023), indicating a Neoproterozoic age for the mafic protolith of the metabasites. Variscan K-Ar ages (348.1–311.4 Ma) reflect cataclasis and mica recrystallization, with phengite composition (Table 2) suggesting pressures of ~12.5 kbar. Such a pressure is not unique in the metamorphic exotic rocks from the Outer Carpathians Ridges. After recalculation of our earlier data (Kania and Wolska, 2009) for the gneissic exotics from the Cisna Beds in the Dukla Unit, according to the formula by Kamzolkin et al. (2016), we obtained pressures between 9.9–14.5 kbar (assuming 500°C temperature). The tectonized Fore-Magura Ridge likely supplied these blocks to the Magura Basin olistostrome. During the sedimentation of the Pasierbiec Sandstone in the middle Eocene, the Fore-Magura Ridge was partly emergent from the basin and eroded. On the southern slopes of the Fore-Magura Ridge, mass movements occurred, facilitating the transport of material into the basin. Large-scale mass movements led to the formation of olistostromes (e.g., Cieszkowski et al., 2009, 2012; Ślączka et al., 2012) within the Pasierbiec Formation. One of these olistostromes contains the olistolith investigated (Cieszkowski et al., 2017).

CONCLUSIONS

The metabasite olistoliths in Osielec, within the Pasierbiec Sandstone Formation, are unique for the Polish Outer Western Carpathians. They represent fragments of a supra-subduction zone ophiolite sequence, characterized by high Fe_2O_3, TiO_2, Al_2O_3, Cr, Ni, Co, V, and display a mixed calc-alkaline/tholeiitic signature due to hybridisation of magma different from that of typical ophiolites. U-Pb zircon dating establishes a Neoproterozoic protolith age (611.7 ±4.7 Ma), while Variscan metamorphism and deformation (348.1–311.4 Ma) are documented by K-Ar phengite ages. Phengite geobarometry revealed pressures 12 kbar. The metabasite of the olistoliths was probably derived from the Fore-Magura Ridge.

This work is dedicated to Prof. Tadeusz Wieser (1922–2005), a distinguished Polish mineralogist and petrologist (Żabiński, 2005).

Author Contributions: Conceptualization: Cieszkowski M., Wolska A., Szczęch M., Kania M., Ślączka A.; **Investigation and Writing – Original Draft:** Cieszkowski M., Wolska A., Szczęch M., Kania M., Ślączka A., Anczkiewicz R., Szczerba M., Ciesielska Z.; **Writing – Review** and **Editing:** Kania M., Szczęch M. All authors reviewed and approved the final manuscript.

Funding

Funded by Pedagogical University in Krakow (BS/452/G/2018) and the Institute of Geological Sciences, Jagiellonian University.

REFERENCES

Anczkiewicz, A.A., Anczkiewicz, R., 2016. U-Pb zircon geochronology and anomalous Sr-Nd-Hf isotope systematics of late orogenic andesites: Pieniny Klippen Belt, Western Carpathians, South Poland. Chemical Geology, **427**: 1–16; https://doi.org/https://doi.org/10.1016/j.chemgeo.2016.02.004

Anczkiewicz, R., Cieszkowski, M., Szczęch, M., Wolska, A., 2016. Ophiolite from Osielec – Magura Nappe, Outer Carpathians, Poland – a new approach to the problem. In: Abstract Book, 10th ESSEWECA Conference 1st – 2nd December 2016, Bratislava, Slovakia (ed. M. Šujan): 9–10.

Anczkiewicz, R., Cieszkowski, M., Szczęch, M., Ślączka, A., Wolska, A., 2018. A new approach to the problem of the ophiolite from Osielec – Magura Nappe, Outer Carpathians, Poland. In: Geologica Balcanica, XXI International Congress of the Carpathian Balkan Geological Association (CBGA), Abstracts, September 10–13, 2018, (eds. F. Neubauer, U. Brendel and G. Friedl): 108. University of Salzburg, Austria.

Birkenmajer, K., 1986. Stages of structural evolution of the Pieniny Klippen Belt, Carpathians. Studia Geologica Polonica, **88**: 7–32.

Bojdys, G., Bujnowski, W., Karaczun, K., Lemberger, M., 1982. Interpretation of gravimetric and magnetic investigations in the Upper Silesian Coal Basin (in Polish with English summary). Biuletyn Instytutu Geologicznego, **333**: 61–90.

Bónová, K., Spišak, K.J., Bóna, J., Kováčik, M., 2017. Chromian spinels from the Magura Unit (Western Carpathians, Eastern Slovakia) – their petrogenetic and palaeogeographic implications. Geological Quarterly, **61** (1): 3–18; https://doi.org/10.7306/gq.1292

Buła, Z., Habryn, R., Jachowicz-Zdanowska, M., Żaba, J., 2015. The Precambrian and Lower Paleozoic of the Brunovistulicum (eastern part of the Upper Silesian Block, southern Poland) – the state of the art. Geological Quarterly, **59** (1): 123–134; https://doi.org/10.7306/gq.1203

Burtan, J., Szymakowska, F., 1966. Szczegółowa Mapa Geologiczna Polski 1:50 000, arkusz Osielec, wydanie tymczasowe (in Polish). Instytut Geologiczny, Warszawa.

Cieszkowski, M., Golonka, J., Krobicki, M., Ślączka, A., Oszczypko, N., Waśkowska-Oliwa, A., Wendorff, M., 2009. The Northern Carpathians plate tectonic evolutionary stages and origin of olistolites and olistostromes. Geodinamica Acta, **22**: 101–126; https://doi.org/10.3166/ga.22.101-126

Cieszkowski, M., Kysiak, T., Ślączka, A., Wolska, A., 2010. Olistoliths of gabbro from Osielec (Magura Nappe, Outer Carpathians, Poland). Geovestník, Mineralia Slovaca, **42**: 507–508.

Cieszkowski, M., Golonka, J., Ślączka, A., Waśkowska, A., 2012. Role of the olistostromes and olistoliths in tectonostratigraphic evolution of the Silesian Basin in the Outer West Carpathians. Tectonophysics, **568**: 248–265; https://doi.org/10.1016/j.tecto.2012.01.030

Cieszkowski, M., Kysiak, T., Szczęch, M., Wolska, A., 2017. Geology of the Magura Nappe in the Osielec area with emphasis on an Eocene olistostrome with metabasite olistoliths (Outer Carpathians, Poland). Annales Societatis Geologorum Poloniae, **87**: 169–182; https://doi.org/10.14241/asgp.2017.009

Condie, K.C., 2005. High field strength element ratios in Archean basalts: a window to evolving sources of mantle plumes? Lithos, **79**: 491–504; https://doi.org/10.1016/j.lithos.2004.09.014

Deer, W.A., Zussman, J., Howie, R.A., 1962. Rock-forming Minerals, **3**, Sheet Silicates. Longmans.

Deer, W.A., Howie, R.A., Zussman, J., 2001. Rock-forming minerals. Vol. 4A, Framework silicates: feldspars (2nd ed.). Geological Society of London.

Dudek, A., 1980. The crystalline basement block of the Outer Carpathians in Moravia: Bruno-Vistulicum. Rozpravy Česko-Slovenské Akademie Věd, Řada Matematicko-přírodních Věd, **90**: 1–85.

Escola, P., 1939. Die metamorphe Gesteine. In: Die Entstehung der Gesteine (eds. T.F.W. Barth, C.W. Correns and P. Escola). Springer, Berlin.

Floyd, P.A., Winchester, J.A., 1975. Magma type and tectonic setting discrimination using immobile elements. Earth and Planetary Science Letters, **27**: 211–218; https://doi.org/10.1016/0012-821X(75)90031-X

Gawęda, A., Golonka, J., Waśkowska, A., Szopa, K., Chew, D., Starzec, K., Wieczorek, A., 2019. Neoproterozoic crystalline exotic clasts in the Polish Outer Carpathian flysch: remnants of the Proto-Carpathian continent? International Journal of Earth Sciences, **108**: 1409–1427; https://doi.org/10.1007/s00531-019-01713-x

Gawęda, A., Szopa, K., Waśkowska, A., Golonka, J., Krzykawski, T., Kalinichenko, T., 2023. Neoproterozoic ophiolite exotic blocks in the Outer Western Carpathians, southern Poland: a record of the fast ocean-floor cooling and alterations. Geological Quarterly, **67**, 9; https://doi.org/10.7306/gq.1679

Golonka, J., Waśkowska, A., Ślączka, A., 2019. The Western Outer Carpathians: origin and evolution. Zeitschrift der Deutschen Gesellschaft für Geowissenschaften, **170**: 229–254; https://doi.org/10.1127/zdgg/2019/0193

Holland, T., Blundy, J., 1994. Non-ideal interactions in calcic amphiboles and their bearing on amphibole-plagioclase thermometry. Contribution to Mineralogy and Petrology, **116**: 433–447.

Jackson, S., Pearson, N., Griffin, W., Belousova, E., 2004. The application of laser ablation-inductively coupled plasma-mass spectrometry to in situ U-Pb zircon geochronology. Chemical Geology, **211**: 47–69; https://doi.org/10.1016/j.chemgeo.2004.06.017

Kamzolkin, V. A., Ivanov, S. D., Konilov, A. N., 2016. Empirical Phengite Geobarometer: Background, Calibration, and Application. Geology of Ore Deposits, **58**: 613–622; https://doi.org/10.1134/S1075701516080092

Kania, M., Wolska, A., 2009. Deformation structures in the gneissic exotic pebbles from the area of Wołosate (Cisna sandstone, Dukla tectonic unit, Outer Carpathians, Poland). Annales Societatis Geologorum Poloniae, **79**: 41–52.

Kellett, D., Joyce, N., 2014. Analytical details of single- and multicollection $^{40}Ar/^{39}Ar$ measurements for conventional step-heating and total-fusion age calculation using the Nu Noblesse at the Geological Survey of Canada. Geological Survey of Canada, Technical Note, **8**.

Koszarski, L., Sikora, W., Wdowiarz, S., 1974. The Flysch Carpathians. Polish Carpathians. In: Tectonics of the Carpathian-Balkan Regions (ed. M. Mahel): 180–197. Geologický ústav Dionýza Štúra, Bratislava.

Koszowska, E., Wolska, A., Zuchiewicz, W., Cuong, N. Q., Pécskay, Z., 2007. Crustal contamination of Late Neogene basalts in the Dien Bien Phu Basin, NW Vietnam: some insights from petrological and geochronological studies. Journal of Asian Earth Sciences, **29**: 1–17; https://doi.org/10.1016/j.jseaes.2005.12.003

Kotas, A., 1985 Uwagi o ewolucji strukturalnej Górnośląskiego Zagłębia Węglowego. In: Tektonika Górnośląskiego Zagłębia Węglowego (eds. J. Trzepierczyńskij): 17–46. Materiały Konferencji Naukowej, Sosnowiec, Wydawnictwo Uniwersytetu Śląskiego, Katowice.

Książkiewicz, M., 1962. Cretaceous and Early Tertiary in the Polish External Carpathians. In: Geological Atlas of Poland. Stratigraphic and Facial Problems (ed. M. Książkiewicz). Instytut Geologiczny, Warszawa.

Książkiewicz, M., 1966. Geologia regionu babiogórskiego (in Polish). In: Przewodnik XXXIX Zjazdu Polskiego Towarzystwa Geologicznego, Babia Góra (ed. M. Książkiewicz): 5–58. Wydaw. Geol., Warszawa.

Książkiewicz, M., 1977. The tectonics of the Carpathians. In: Geology of Poland, Volume **IV**, Tectonics, The Alpine Tectonic Epoch (ed. W. Pożaryski): 476–620. Wydaw. Geol., Warszawa.

Książkiewicz, M., Rączkowski, W., Wójcik, A., 2017. Szczegółowa Mapa Geologiczna Polski 1:50 000, arkusz Osielec (1015) (in Polish). Państw. Inst. Geol. – PIB, Warszawa.

Kuno, H., 1960. High-alumina basalt. Journal of Petrology, **1**: 121–145; https://doi.org/10.1093/petrology/1.1.121

Leake, B.E., 1964. The chemical distinction between otho- and para-amphibolites. Journal of Petrology, **5**: 238–255.

Leake, B.E., Woolley, A.R. Arps C.E.S., Birch, W.D., Gilbert, M.C., Grice, J.D., Hawthorne, F.C., Kato, A., Kisch, H.J., Krivovichev, V.G., Lintohout, K., Laird, J., Mandarino, J., Maresch, W.V., Nickel, E.H., Rock, N.M.S., Schumacher, J.C., Smith, D.C., Stephenson, N.C.N., Ungaretti, L., Whittaker, E.J.W., Youzhi, G., 1997. Nomenclature of amphiboles: Report of the subcommittee on amphiboles of the international mineralogical association, commission on new minerals and mineral names. American Mineralogist, **82**: 295–310; https://doi.org/10.1180/minmag.1997.061.405.13

Leardi, L., Rossetti, P., Crisci, G.M., 1986. Greenschist altered metabasalt (ovardite) from Torre d'Ovarda (Val d'Ala, Graian Alps). Ofioliti, **11**: 263–274.

Lee, D., Severn, G., Oksuz, L., Hershkowitz, N., 2006. Laser-induced fluorescence measurements of argon ion velocities near the sheath boundary of an argon–xenon plasma. Journal of Physics D: Applied Physics, **39,** 5230; https://doi.org/10.1088/0022-3727/39/24/020

Ludwig, K.R., 2008. Users Manual for Isoplot/Ex. Berkeley Geochronology Center Special Publication, **4**: 77.

Miyashiro, A., Shido, F., 1975. Tholeiitic and clac-alkaline series in relations to the behaviors of titanium, vanadium, chromium, and nickel. American Journal of Science, **275**: 265–277.

Niggli, P., 1948. Gesteine und Minerallagerstätten. Birkhäuser, Basel.

Odin, G.S., 1982. Interlaboratory standards for dating purposes. In Numerical dating in stratigraphy (ed. G.S. Odin): 123–149. Wiley and Sons, Chichester.

Oszczypko, N., 1992. Late Cretaceous through Paleogene evolution of Magura Basin. Geologica Carpathica, **43:** 333–338.

Oszczypko, N., Salata, D., 2005. Provenance analyses of the Late Cretaceous: Palaeocene deposits of the Magura Basin (Polish Western Carpathians) : evidence from the heavy minerals study. Acta Geologica Polonica, **55**: 237–267.

Oszczypko, N., Ślączka, A., Oszczypko-Clowes, M., Olszewska, B., 2015. Where was the Magura Ocean? Acta Geologica Polonica, **65**: 319–344; https://doi.org/10.1515/agp-2015-0014

Passchier, C.W., Trouw, R.A.J., 2005. Microtectonics. Springer Science & Business Media.

Paton, C., Woodhead, J., Hellstrom, J., Hergt, J., Greig, A., Maas R., 2010. Improved laser ablation U-Pb zircon geochronology through robust downhole fractionation correction. Geochemistry, Geophysics, Geosystems, **11**, Q0AA06; https://doi.org/10.1029/2009GC002618

Paton, C., Hellstrom, J., Paul, B., Woodhead, J., Hergt, J., 2011. Iolite: Freeware for the Visualisation and Processing of Mass Spectrometric Data. Journal of Analytical Atomic Spectrometry, **26**: 2508–2518; https://doi.org/10.1039/C1JA10172B

Pearce, J.A., 1983. Role of the sub-continental lithosphere in magma Genesis at active Continental margins. In: Continental Basalts and Mantle Xenotiths, Shiva Cheshire, UK (eds. C.J. Hawkesworth and M.J. Norry): 230–249.

Pearce, J.A., 1996. A user's guide to basalt discrimination diagrams. Geological Association of Canada, Short Course Notes, **12:** 79–113.

Picha, F.J., Stránik, Z., Krejči, O., 2006. Geology and hydrocarbon resources of the Outer Western Carpathians and their foreland, Czech Republic. AAPG Memoir, **84**: 49-175; https://doi.org/ 10.1306/985607M843067

Robinson, P., Spear, F.S., Schumacher, J.C., Laird, J., Klein, C., Evans, B.W., Doolan, B.L., 1982. Phase relations of metamorphic amphiboles: natural occurrence and theory. Mineralogical Society of America Reviews in Mineralogy, **9B**.

Shervais, J.W., 2001. Birth, death, and resurrection: The life cycle of suprasubduction zone ophiolites. Geochemistry, Geophysics, Geosystems, **2**, 2000GC000080; https://doi.org/10.1029/2000GC000080

Sláma, J., Košler, J., Condon, D., Crowley, J.L., Gerdes, A., Hanchar, J. M., Horstwood, M.S.A., Morris, G.A., Nasdala, L., Norberg, N., Schaltegger, U., Schoene, B., Tubrett, M.N., Whitehouse, M.J., 2008. Plešovice zircon – a new natural reference material for U-Pb and Hf isotopic microanalysis. Chemical Geology, **249**: 1–35; https://doi.org/10.1016/j.chemgeo.2007.11.005

Smulikowski, W., Desmons, J., Fettes, D.J., Harte, B., Sassi, F., Schmid, R., 2011. Types, grade and facies of metamorphism. In: Metamorphic Rocks: A Classification and Glossary of Terms (eds. D. Fettes and J. Desmons). Cambridge University Press, 16–23.

Sun, S., McDonough, W.F., 1989. Chemical and isotope systematics of oceanic basalts: implications for mantle composition and processes. Geological Society Special Publications, **42**: 313–345; https://doi.org/10.1144/GSL.SP.1989.042.01.19

Ślączka, A., 1971. The geology of the Dukla Unit, Polish Flysch Carpathians (in Polish with English summary). Prace Instytutu Geologicznego, **63**.

Ślączka, A., Kruglov, S., Golonka, J., Oszczypko, N., Popadyuk, I., 2006. The general geology of the Outer Carpathians, Poland, Slovakia, and Ukraine. AAPG Memoir, **84**: 221–258; https://doi.org/10.1306/985610M843070

Ślączka, A., Renda, P., Cieszkowski, M., Golonka, J., Nigro, F., 2012. Sedimentary basins evolution and olistoliths formation: The case of Carpathian and Sicilian regions. Tectonophysics, **568**: 306–319; https://doi.org/10.1016/j.tecto.2012.03.018

Taylor, S.R., McLennan, S.M., 1985. The continental crust: its composition and evolution. Blackwell Scientific Publications (Oxford).

Teťák, F., 2022. Facies analysis of gravity flow deposits of an ancient foreland basin (Magura Nappe, Western Carpathians). Geologica Carpathica, **73**: 545–559; https://doi.org/10.31577/GeolCarp.73.6.5

Tilley, C.E., 1950. Some aspects of magmatic evolution. Quarterly Journal of the Geological Society of London, **106**: 37–61.

Turner, F.J., 1981. Metamorphic Petrology: Mineralogical, Field, and Tectonic Aspects. McGraw-Hill, Washington, New York.

Waśkowska, A., Szczęch, M., Golonka, J., 2025. Composition and stratigraphy of an olistostrome complex in the Eocene deep-sea deposits of the Magura Nappe (Outer Carpathians, Poland). Annales Societatis Geologorum Poloniae, **95**: 63–83.

Wiedenbeck, M., Allé, P., Corfu, F., Griffin, W. L., Meier, M., Oberli, F., Von Quadt, A., Roddick, J. C., Spiegel, W., 1995. Three natural zircon standards for U-Th-Pb, Lu-Hf, trace element and REE analyses. Geostandards Newsletter, **19**: 1–23; https://doi.org/10.1111/j.1751-908X.1995.tb00147.x

Wieser, T., 1952. The ophiolite from Osielec (in Polish with English summary). Annales Societatis Geologorum Poloniae, **21**: 319–327.

Wieser, T., 1966. On the petrography of the Babia Góra Region (in Polish). In: Przewodnik XXXIX Zjazdu Polskiego Towarzystwa Geologicznego, Babia Góra, 2–5 czerwca 1966 (ed. M. Książkiewicz): 91–100. Wydaw. Geol., Warszawa.

Wójcik, A., Rączkowski, W., 1994. Objaśnienia do Szczegółowej Mapy Geologicznej Polski 1:50 000, arkusz Osielec (1015) (in Polish). Państw. Inst. Geol., Warszawa.

Żaba, J., 1999. The structural evolution of Lower Palaeozoic succession in the Upper Silesia Block and Małopolska Block border zone (Southern Poland) (in Polish with English summary). Prace Państwowego Instytutu Geologicznego, **166**.

Żabiński, W., 2005. Tadeusz Wieser (1922–2005). Mineralogia Polonica, **36**: 67–68.

Żelaźniewicz, A., Buła, Z., Fanning, M., Seghedi, A., Żaba, J., 2009. More evidence on Neoproterozoic terranes in Southern Poland and southeastern Romania. Geological Quarterly, **58** (1): 93–124.

Żelaźniewicz, A., Aleksandrowski, P., Buła, Z., Karnkowski, P. H., Konon, A., Oszczypko, N., Ślączka, A., Żaba, J., Żytko, K., 2011. Regionalizacja Tektoniczna Polski (in Polish). Komitet Nauk Geologicznych PAN, Wrocław.